Continuous symmetry breaking of low-dimensional systems driven by inhomogeneous oscillatory driving forces

Harukuni Ikeda ⬤*

Department of Physics, Gakushuin University, 1-5-1 Mejiro, Toshima-ku, Tokyo 171-8588, Japan

Yuta Kuroda ⬤

Department of Physics, Nagoya University, Nagoya 464-8602, Japan

The driving forces of chiral active particles and deformations of cells are often modeled by spatially inhomogeneous but temporally periodic driving forces. Such inhomogeneous oscillatory driving forces have only recently been proposed in the context of active matter, and their effects on the systems are not yet fully understood. In this work, we theoretically study the impact of spatially inhomogeneous oscillatory driving forces on continuous symmetry breaking. We first analyze the linear model for the soft modes in the ordered phase to derive the lower critical dimension of the model, and then analyze the spherical model to investigate more detailed phase behaviors. Interestingly, our analysis reveals that symmetry breaking occurs even in one and two dimensions, where the Hohenberg-Mermin-Wagner theorem prohibits continuous symmetry breaking in equilibrium. Furthermore, fluctuations of conserved quantities, such as density, are anomalously suppressed in the long-wavelength, i.e., show hyperuniformity.

I. INTRODUCTION

As the temperature is lowered, gas becomes liquid and then liquid becomes solid. These dramatic changes in physical properties are called phase transitions [1]. The phase transitions in equilibrium systems have been actively studied using powerful tools of statistical mechanics such as the renormalization groups [2], scaling theories [3], exact solutions [4,5], and extensive numerical simulations [6–8]. The phase transitions in nonequilibrium systems are also actively investigated, though the theoretical development is still in its infancy compared to that of the equilibrium phase transitions.

One of the most well-known no-go theorems in the theory of equilibrium phase transitions is the Hohenberg-Mermin-Wagner theorem [9,10]. This theorem claims that short-range interacting systems having continuous degrees of freedom do not show long-range order in one and two dimensions. However, the theorem does not hold for nonequilibrium systems, and indeed there are several examples of low-dimensional systems showing tlong-range order. Examples include the *XY* model driven by anisotropic noise [11,12], $O(n)$ model driven by shear [13–15], and models driven by anticorrelated noise [16,17], polar active fluids [18–20], and nonreciprocal systems [21,22].

A popular class of nonequilibrium systems is periodically driven systems. For instance, spin systems in an ac field have been investigated extensively to understand hysteresis of ferromagnets [23–26]. Other examples include tapping experiments of granular systems [27] and emulsions subjected to an oscillatory shear strain [28,29]. In the above examples,

the systems are driven by the spatially *homogeneous* driving force. For instance, in a typical setting of magnetic hysteresis, all spins $i = 1, \ldots, N$ are driven by the same external field such as $h_i(t) = h(t) = a \sin(\omega_0 t)$, where a and ω_0 denote the strength and frequency of the driving force, respectively. Recently, a different type of driving force was proposed in the context of active matter, namely, spatially *inhomogeneous* but temporally periodic driving forces [30]. For instance, tissues are often driven by oscillatory deformations of constituent cells [31,32]. To model this behavior, Tjhung and Berthier introduced a model consisting of actively deforming particles [32]. The diameter σ_i of the *i*th particle of the model oscillates around its mean value σ_i^0 as follows:

$$\sigma_i(t) = \sigma_i^0[1 + a \cos(\omega_0 t + \psi_i)], \quad (1)$$

where a and ω_0 denote the strength and frequency of the oscillation, respectively, and ψ_i denotes a random phase shift [32]. When $\psi_i = 0$, Eq. (1) represents the affine compression or decompression, while, when $\psi \neq 0$, it leads to spatially inhomogeneous deformations. Another example of inhomogeneous driving force appears in chiral active matter, where constituent particles spontaneously rotate due to the periodic nature of the driving force [33,34]. A popular numerical model to describe the rotational motion of a chiral active particle in two dimensions is [35]

$$\dot{x}_i = -\frac{\partial V}{\partial x_i} + h \cos\theta_i + \xi_{i,x},$$

$$\dot{y}_i = -\frac{\partial V}{\partial y_i} + h \sin\theta_i + \xi_{i,y}, \quad (2)$$

$$\dot{\theta}_i = \omega_0 + \xi_\theta,$$

---

*Contact author: harukuni.ikeda@gakushuin.ac.jp

where (x_i, y_i) denotes the position of the ith particle, $\xi_{i,x,y,\theta}$ denotes the noise, and V denotes the interaction potential. In the absence of noise $\xi_{i,x,y,\theta} = 0$, the equations are reduced to

$$\dot{x}_i = -\frac{\partial V}{\partial x_i} + h_{i,x}, \quad \dot{y}_i = -\frac{\partial V}{\partial y_i} + h_{i,y}. \tag{3}$$

Here the particle is driven by the inhomogeneous driving force $h_{i,x} = h\cos(\omega_0 t + \psi_i)$ and $h_{i,y} = h\sin(\omega_0 t + \psi_i)$, where the phase shift ψ_i is determined by the initial condition $\psi_i = -\omega_0 t_{\text{ini}} + \theta_i(t_{\text{ini}})$. The phase behavior of this type of system, including actively deforming particles and chiral active matter, was studied recently [32,36–42]. However, the effects of the inhomogeneous driving force on the phase transition have not been fully understood yet.

This study focuses on continuous symmetry breakings such as crystallization and nematic transition systems driven by inhomogeneous oscillatory driving forces. In particular, we show that continuous symmetry-breaking can occur even in low dimensions $d \leqslant 2$ for systems driven solely by inhomogeneous oscillatory driving forces. To achieve this goal, we first investigate the linear model and derive the lower critical dimension. Here we only assume that the model has at least one massless mode in the ordered phase, and thus, the result should be applied for general types of continuous symmetry breaking such as crystallization and nematic phase transitions. Next, we investigate the spherical model to discuss more detailed phase behaviors [1,43].

The spherical model was first introduced by Berlin and Kac as a simplification of the Ising model [44]. The model can be solved analytically in any dimension, both in equilibrium and nonequilibrium [1,45,46]. In equilibrium, the model undergoes the second-order phase transition from the paramagnetic to the ferromagnetic phase at finite temperatures. The critical exponents of the transition agree with those of the $n \to \infty$ limit of the $O(n)$ model [1]. In previous studies, the spherical model driven by the homogeneous oscillatory driving forces was investigated extensively in the context of the magnetic hysteresis [23–26] and also structural glasses [29].

The structure of the paper is as follows. In Sec. II, we investigate the linear model by using the scaling analysis. In Sec. III, we investigate the spherical model. In Sec. IV, we briefly discuss the behavior of the conserved order parameter such as density. In particular, we show that the fluctuations of the conserved quantity are highly suppressed, implying that the model exhibits hyperuniformity [47]. In Sec. V, we conclude the work.

II. LINEAR MODEL

When continuous symmetries are spontaneously broken, there arise soft modes called the Nambu-Goldstone (NG) modes [48,49]. In equilibrium, the fluctuations of NG modes diverge in $d \leqslant 2$, which destroys the long-range order. Therefore, continuous symmetries are not spontaneously broken for $d \leqslant 2$ in equilibrium systems. This fact is nowadays widely known as the Hohenberg-Mermin-Wagner theorem [9,10]. We here investigate the scaling behavior of the NG modes to discuss the stability of the ordered phase of systems driven by inhomogeneous oscillatory driving forces. Let u be the

displacement along one of the NG modes. We assume that u follows the following phenomenological linear equation:

$$\frac{\partial u(\boldsymbol{x}, t)}{\partial t} = \nabla^2 u(\boldsymbol{x}, t) + f(\boldsymbol{x}, t), \tag{4}$$

$$f(\boldsymbol{x}, t) = \xi(\boldsymbol{x}, t) + h(\boldsymbol{x}, t), \tag{5}$$

where $\xi(\boldsymbol{x}, t)$ denotes a Gaussian white noise satisfying

$$\langle \xi(\boldsymbol{x}, t) \rangle = 0,$$
$$\langle \xi(\boldsymbol{x}, t)\xi(\boldsymbol{x}', t') \rangle = 2T\delta(\boldsymbol{x} - \boldsymbol{x}')\delta(t - t'), \tag{6}$$

and $h(\boldsymbol{x}, t)$ represents an inhomogeneous oscillatory driving force

$$h(\boldsymbol{x}, t) = \sqrt{2D}\cos[\omega_0 t + \psi(\boldsymbol{x})]|d\boldsymbol{x}|^{-1/2}, \tag{7}$$

where $|d\boldsymbol{x}|$ denotes the volume of the unit cell of the discretization. T and D stand for the strength of the noise and the driving force, respectively. In Eq. (7), we introduce the random phase shift $\psi(\boldsymbol{x})$ distributed uniformly in $[0, 2\pi]$ [30]. The case with $\psi(\boldsymbol{x}) = 0$ corresponds to a homogeneous driving force. The mean and variance of $h(\boldsymbol{x}, t)$ are [50]

$$\langle h(\boldsymbol{x}, t) \rangle = 0,$$
$$\langle h(\boldsymbol{x}, t)h(\boldsymbol{x}', t') \rangle = D\delta(\boldsymbol{x} - \boldsymbol{x}')\cos[\omega_0(t - t')], \tag{8}$$

where we use $\delta(\boldsymbol{x} - \boldsymbol{x}') = \lim_{|d\boldsymbol{x}| \to 0} \delta_{\boldsymbol{x},\boldsymbol{x}'}/|d\boldsymbol{x}|$ in the continuum limit. In Eqs. (6) and (8), the symbol $\langle \bullet \rangle$ represents either the average over the noise ξ or the randomness ψ. Equation (8) implies that the time translational symmetry is restored after taking the average for the quenched randomness $\psi(\boldsymbol{x})$. To investigate the scaling behavior, we consider the following scaling transformation [19,51]:

$$x \to bx, \ t \to b^z t, \ u \to b^\chi u. \tag{9}$$

To calculate the scaling dimension of the driving force $f(\boldsymbol{x}, t)$, we observe the fluctuation induced by $f(\boldsymbol{x}, t)$ in $d + 1$-dimensional Euclidean space $[0, l]^d \times [0, t]$ [47]

$$\sigma(l, t) = \left\langle \left(\int_{\boldsymbol{x}' \in [0,l]^d} d\boldsymbol{x}' \int_0^t dt' f(\boldsymbol{x}', t') \right)^2 \right\rangle$$
$$= \sigma_\xi(l, t) + \sigma_h(l, t), \tag{10}$$

where

$$\sigma_\xi(l, t) = \left\langle \left(\int_{\boldsymbol{x}' \in [0,l]^d} d\boldsymbol{x}' \int_0^t dt' \xi(\boldsymbol{x}', t') \right)^2 \right\rangle,$$

$$\sigma_h(l, t) = \left\langle \left(\int_{\boldsymbol{x}' \in [0,l]^d} d\boldsymbol{x}' \int_0^t dt' h(\boldsymbol{x}', t') \right)^2 \right\rangle. \tag{11}$$

For $T > 0$ and $\omega_0 \neq 0$, we get $\sigma_\xi \sim l^d t$ and $\sigma_h \sim l^d t^0$, leading to $\sigma \sim \sigma_\xi \sim l^d t$ for $l \gg 1$ and $t \gg 1$. Since $\sigma \sim t^2 l^{2d} f^2$, we have $f(\boldsymbol{x}, t) \to b^{-z/2} b^{-d/2} f(\boldsymbol{x}, t)$ for $T > 0$ and $\omega_0 \neq 0$. On the contrary, for $T = 0$ and $\omega_0 \neq 0$, we get $\sigma = \sigma_h \sim l^d t^0$, leading to $f(\boldsymbol{x}, t) \to b^{-z} b^{-d/2} f(\boldsymbol{x}, t)$. For $\omega_0 = 0$, $h(\boldsymbol{x}, t) \propto \cos\psi(\boldsymbol{x})$ is a time-independent constant force, which leads to the ballistic behavior $\sigma \sim \sigma_h \sim l^d t^2$. Therefore, we get $f(\boldsymbol{x}, t) \to b^{-d/2} f(\boldsymbol{x}, t)$ for $\omega_0 = 0$. In summary, after the scal-

ing transformation, Eq. (4) reduces to

$$
b^{\chi-z}\frac{\partial u(\boldsymbol{x},t)}{\partial t} = b^{\chi-2}\nabla^2 u(\boldsymbol{x},t) + b^{z_f}f(\boldsymbol{x},t),
$$

$$
z_f = \begin{cases} -\frac{z}{2}-\frac{d}{2} & T>0, \quad \omega_0 \neq 0 \\ -z-\frac{d}{2} & T=0, \quad \omega_0 \neq 0, \\ -\frac{d}{2} & \omega_0 = 0. \end{cases} \quad (12)
$$

Assuming all terms have the same scaling dimension, we get the following scaling relations [1,52]:

$$
\chi - z = \chi - 2 = z_f, \quad (13)
$$

leading to

$$
z = 2,
$$

$$
\chi = \begin{cases} 1-\frac{d}{2} & T>0, \quad \omega_0 \neq 0, \\ -\frac{d}{2} & T=0, \quad \omega_0 \neq 0, \\ 2-\frac{d}{2} & \omega_0 = 0. \end{cases} \quad (14)
$$

To see the stability of the ordered phase, we observe the fluctuations of the NG modes [19]

$$
\langle \delta u^2 \rangle \sim b^{2\chi}. \quad (15)
$$

For the ordered phase to be stable, χ must be negative; otherwise, the fluctuations diverge in the thermodynamic limit $b \to \infty$, and the long-range order is destroyed [19]. Therefore, the lower-critical dimension can be determined by setting $\chi = 0$:

$$
d_l = \begin{cases} 2 & T>0, \quad \omega_0 \neq 0, \\ 0 & T=0, \quad \omega_0 \neq 0, \\ 4 & \omega_0 = 0. \end{cases} \quad (16)
$$

The above equation is the main result of this paper. For $T>0$ and $\omega_0 \neq 0$, we get $d_l = 2$, as in equilibrium [9,10], meaning that the periodic driving forces do not change the lower critical dimension at finite T. On the contrary, for $T=0$ and $\omega_0 \neq 0$, we get $d_l = 0$, meaning that the long-range order can appear even in $d=1$ and $d=2$. For $\omega_0 = 0$, we get $d_l = 4$. This is natural since $h(\boldsymbol{x},t) \propto \cos\psi(\boldsymbol{x})$ plays the role of the random field, which destroys the order in the systems with continuous symmetry for $d \leqslant 4$ according to the Imry-Ma arguments [1,53]. Equation (16) should also be applied for an arbitrary function $h(\boldsymbol{x},t)$ that is temporally periodic and spatially uncorrelated for which $\sigma_h \sim l^{d/2}t^0$.

The argument so far is phenomenological but quite general, where we only assume the existence of the NG modes. Equation (16) should be applied for general types of continuous symmetry breaking such as the ferromagnetic phase transition of the $O(n)$ model with $n \geqslant 2$, crystalization, and nematic phase transition.

However, the above linear model cannot describe the phase transitions. To investigate the phase behaviors more closely, in the next section, we investigate the mean-spherical model [44], which corresponds to the $n \to \infty$ limit of the $O(n)$ model and can be solved exactly [1].

III. SPHERICAL MODEL

For concreteness, we here introduce and investigate the mean-spherical model and discuss more detailed phase behaviors. Let $\phi(\boldsymbol{x},t)$ be a nonconserved order parameter such

as the magnetization. We assume that the time evolution of $\phi(\boldsymbol{x},t)$ follows the model-A dynamics [54]

$$
\frac{\partial \phi(\boldsymbol{x},t)}{\partial t} = -\frac{\delta \mathcal{F}[\phi]}{\delta\phi(\boldsymbol{x},t)} + f(\boldsymbol{x},t), \quad (17)
$$

where the driving force $f(\boldsymbol{x},t)$ is defined by Eq. (5). The free-energy $\mathcal{F}[\phi]$ of the mean-spherical model is defined as [17,55]

$$
\mathcal{F}[\phi] = \int d\boldsymbol{x}\left[\frac{(\nabla\phi)^2}{2} + \frac{\mu\phi^2}{2}\right], \quad (18)
$$

where μ denotes the Lagrange multiplier to impose the mean-spherical constraint

$$
\int d\boldsymbol{x}\langle\phi(\boldsymbol{x})^2\rangle = N. \quad (19)
$$

The model is studied extensively in equilibrium $D=0$, where the critical exponents agree with those of the large n limit of the $O(n)$ model [1,46]. Below we investigate the phase behaviors of the model in the thermodynamics limit: $N \to \infty$ and $\int d\boldsymbol{x} = V \to \infty$ with fixed ratio $\rho = N/V$.

We shall make some comments on μ. Equation (17) is written as

$$
\frac{\partial \phi(\boldsymbol{x},t)}{\partial t} = -(\mu - \nabla^2)\phi(\boldsymbol{x},t) + f(\boldsymbol{x},t). \quad (20)
$$

By integrating Eq. (20) with regard to (w.r.t.) $\boldsymbol{x}$, we get $\dot{m}(t) = -\mu\mathrm{m}(t)$, where $m(t) = V^{-1}\int d\boldsymbol{x}\phi(\boldsymbol{x},t)$. The Lagrange multiplier should satisfy $\mu \geqslant 0$ since, otherwise, the steady state becomes unstable. In the steady state $\dot{m} = -\mu m = 0$. This condition is automatically satisfied in the disordered phase $m=0$. In the ordered phase $m>0$, on the contrary, μ should vanish $\mu = 0$. Therefore, in the ordered phase Eq. (20) reduces to the linear equation Eq. (4) analyzed in the previous section. As a consequence, the lower critical dimension d_l of the mean-spherical model is given by Eq. (16), as we will confirm later.

We decompose the order parameter $\phi(\boldsymbol{x},t)$ into the mean value m and fluctuations $\tilde{\phi}(\boldsymbol{x},t) \equiv \phi(\boldsymbol{x},t) - m$. Since $\dot{m} = -\mu m = 0$ in the steady state, $\tilde{\phi}(\boldsymbol{x},t)$ satisfies the same equation as Eq. (20). Thus, the Fourier transform of the equation leads to

$$
i\omega\tilde{\phi}(\boldsymbol{q},\omega) = -(q^2+\mu)\tilde{\phi}(\boldsymbol{q},\omega) + f(\boldsymbol{q},\omega), \quad (21)
$$

where $q = |\boldsymbol{q}|$ and

$$
\tilde{\phi}(\boldsymbol{q},\omega) = \int d\boldsymbol{x}dt e^{-i\boldsymbol{q}\cdot\boldsymbol{x}-i\omega t}\tilde{\phi}(\boldsymbol{x},t). \quad (22)
$$

From Eq. (21), we get

$$
\tilde{\phi}(\boldsymbol{q},\omega) = \frac{f(\boldsymbol{q},\omega)}{i\omega + (q^2+\mu)}. \quad (23)
$$

The two-point correlation is then calculated as

$$
\langle\phi(\boldsymbol{q},\omega)\phi(\boldsymbol{q}',\omega')\rangle = (2\pi)^{d+1}\delta(\boldsymbol{q}+\boldsymbol{q}')\delta(\omega+\omega')S(\boldsymbol{q},\omega),
$$

$$
(24)
$$

where $\phi(\boldsymbol{q}, \omega)$ denotes the Fourier transform of $\phi(\boldsymbol{x}, t)$, and

$$S(\boldsymbol{q}, \omega) = m^2 (2\pi)^{d+1} \delta(\omega) \delta(\boldsymbol{q}) + \frac{2T}{\omega^2 + (q^2 + \mu)^2}$$
$$+ \frac{D\pi}{\omega_0^2 + (q^2 + \mu)^2} [\delta(\omega + \omega_0) + \delta(\omega - \omega_0)].$$
(25)

The static correlation is obtained by integrating Eq. (25) over ω:

$$S(\boldsymbol{q}) = \frac{1}{2\pi} \int d\omega S(\boldsymbol{q}, \omega)$$
$$= (2\pi)^d m^2 \delta(\boldsymbol{q}) + \frac{T}{q^2 + \mu} + \frac{D}{\omega_0^2 + (q^2 + \mu)^2}. \quad (26)$$

The remaining task is to determine the Lagrange multiplier μ by the spherical constraint

$$N = \int d\boldsymbol{x} \langle \phi(\boldsymbol{x}, t)^2 \rangle = \frac{V}{(2\pi)^d} \int d\boldsymbol{q} S(\boldsymbol{q}). \quad (27)$$

Substituting Eq. (26) into Eq. (27), we get

$$1 = \frac{m^2}{\rho} + TF(\mu) + DG(\mu), \quad (28)$$

where

$$F(\mu) = \frac{\Omega_d}{(2\pi)^d \rho} \int_0^{q_D} \frac{dq q^{d-1}}{q^2 + \mu},$$
$$G(\mu) = \frac{\Omega_d}{(2\pi)^d \rho} \int_0^{q_D} \frac{dq q^{d-1}}{\omega_0^2 + (q^2 + \mu)^2}. \quad (29)$$

Here q_D denotes the phenomenological cutoff, and Ω_d denotes the d-dimensional solid angle.

Now we discuss the phase behavior for finite T. For sufficiently high T, the system is in a disordered phase. As T decreases, the model undergoes a continuous phase transition at a certain point $T = T_c$. Since $\mu = 0$ and $m = 0$ at the transition point, T_c is calculated as

$$T_c = \frac{1 - DG(0)}{F(0)}. \quad (30)$$

For $d \leqslant 2$, $F(0)$ diverges, and thus the phase transition does not occur at finite T. In other words, the lower critical dimension is $d_l = 2$. This is the same situation as that in the equilibrium phase transition, where the Hohenber-Mermin-Wagner theorem prohibits the ordered phase for $d \leqslant 2$ [9,10]. We show T_c in Fig. 1(a).

Next, we discuss the phase behavior in the limit $T \to 0$. For this purpose, it is convenient to control D instead of T. For sufficiently large D, the system is in the disordered phase. With decreasing D, the model undergoes the phase transition at

$$D_c = \frac{1 - TF(0)}{G(0)}. \quad (31)$$

For $T > 0$ and $d \leqslant 2$, $F(0)$ diverges, and thus the ordered phase does not appear. On the contrary, when $T = 0$, D_c can have a finite value $\lim_{T \to 0} D_c = 1/G(0)$ for all $d > 0$, which implies $d_l = 0$ and is consistent with Eq. (16). To visualize

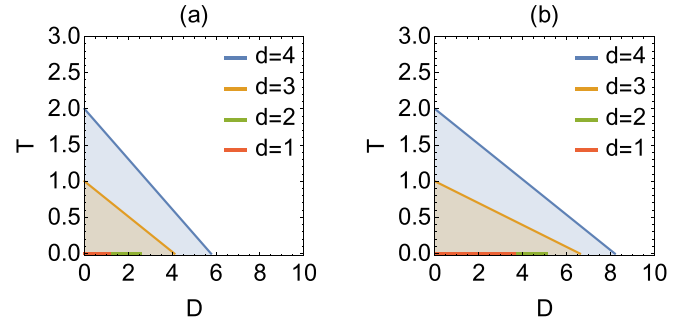FIG. 1. T–D phase diagrams for (a) model-A and (b) model-B. The solid lines denote the critical lines T_c for $d = 4$, 3, 2, and 1 from top to bottom. The filled regions represent the ordered phase. For $d \leqslant 2$, ordered phases appear only at $T = 0$. For simplicity here we set $\rho = \Omega_d/(2\pi)^d$, $q_D = 1$, and $\omega_0 = 1$.

this result, in Fig. 2(a), we show the dimensional dependence of D_c for various temperatures.

Finally, we consider the ω_0 dependence of the phase behavior. For $\omega_0 \neq 0$, all qualitative phase behaviors discussed above remain unchanged. On the contrary, when $\omega_0 = 0$, $G(0)$ diverges for $d \leqslant 4$, leading to $D_c \to 0$ and $T_c \to -\infty$. Therefore, the phase transition does not occur for all $d \leqslant 4$. This is a natural result because $h(\boldsymbol{x}, t)$ for $\omega_0 = 0$ plays the role of a random field, which destroys the long-range order for $d \leqslant 4$ according to the Imry-Ma argument for continuous variables [53]. In Fig. 3(a), we show a D–d phase diagram for various ω_0 to visualize how the ordered phase for $d \leqslant 4$ disappears in the limit $\omega_0 \to 0$. The above result implies $d_l = 4$, which is consistent with the linear model Eq. (16).

IV. CONSERVED ORDER PARAMETER

So far, we discussed the phase behavior for the nonconserved order parameter. Below we discuss what will happen for the conserved order parameter such as density. A conserved quantity $\phi(\boldsymbol{x}, t)$ follows the continuity equation

$$\frac{\partial \phi(\boldsymbol{x}, t)}{\partial t} = -\boldsymbol{\nabla} \cdot \boldsymbol{J}(\boldsymbol{x}, t), \quad (32)$$
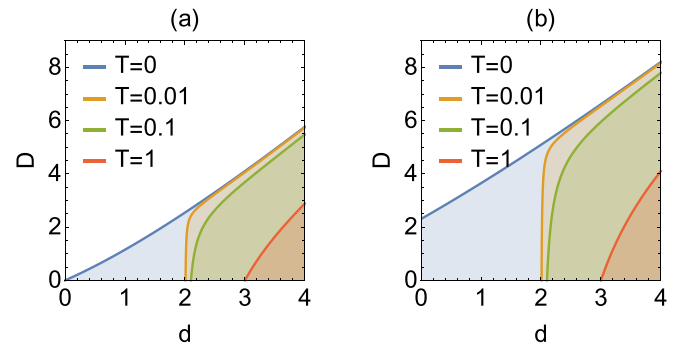

FIG. 2. D–d phase diagrams for (a) model-A and (b) model-B. The solid lines represent D_c for $T = 0$, 0.01, 0.1, and 1 from top to bottom. The filled regions represent the ordered phases. When $T > 0$, the ordered phase appears only if $d > 2$. On the contrary, when $T = 0$, the ordered phase appears for all $d > 0$. For simplicity we here set $\rho = \Omega_d/(2\pi)^d$, $q_D = 1$, and $\omega_0 = 1$.
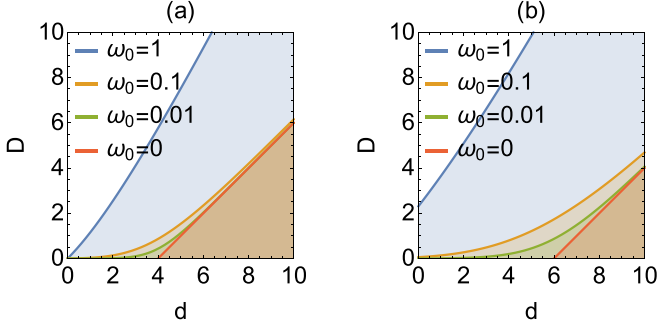
FIG. 3. D–d phase diagrams for $T = 0$ for (a) model-A and (b) model-B. The solid lines denote D_c for $\omega_0 = 1, 0.1, 0.01$, and 0 from top to bottom. The filled regions represent the ordered phases. When $\omega_0 > 0$, the ordered phase appears for all $d > 0$. On the contrary, when $\omega_0 = 0$, the ordered phase appears only when $d > 4$ for the model-A and $d > 6$ for the model-B. For simplicity we here set $\rho = \Omega_d / (2\pi)^d$, $q_D = 1$.

where $\boldsymbol{J}$ denotes the flux. In the model-B dynamics, $\boldsymbol{J}$ is written as [54,56,57]

$$\boldsymbol{J}(\boldsymbol{x}, t) = -\nabla \frac{\delta \mathcal{F}[\phi]}{\delta \phi(\boldsymbol{x}, t)} + \boldsymbol{f}(\boldsymbol{x}, t),$$

$$\boldsymbol{f}(\boldsymbol{x}, t) = \boldsymbol{\xi}(\boldsymbol{x}, t) + \boldsymbol{h}(\boldsymbol{x}, t), \tag{33}$$

where $\mathcal{F}[\phi]$ is the free energy of the mean-spherical model Eq. (18) and $\boldsymbol{\xi} = \{\xi_a\}_{a=1,...,d}$ and $\boldsymbol{h} = \{h_a\}_{a=1,...,d}$ satisfy

$$\langle \xi_a(\boldsymbol{x}, t) \rangle = 0,$$

$$\langle \xi_a(\boldsymbol{x}, t) \xi_b(\boldsymbol{x}', t') \rangle = 2T \delta_{ab} \delta(\boldsymbol{x} - \boldsymbol{x}') \delta(t - t'),$$

$$\langle h_a(\boldsymbol{x}, t) \rangle = 0,$$

$$\langle h_a(\boldsymbol{x}, t) h_b(\boldsymbol{x}', t') \rangle = \delta_{ab} \delta(\boldsymbol{x} - \boldsymbol{x}') D \cos[\omega_0(t - t')]. \tag{34}$$

A calculation very similar to that in the previous section yields

$$S(\boldsymbol{q}) = (2\pi)^d m^2 \delta(\boldsymbol{q}) + \frac{T}{q^2 + \mu} + \frac{Dq^2}{\omega_0^2 + q^4(q^2 + \mu)^2}. \tag{35}$$

When $T = 0$ for $q \neq 0$, we get

$$\lim_{T \to 0} S(\boldsymbol{q}) = \frac{Dq^2}{q^4(q^2 + \mu)^2 + \omega_0^2}. \tag{36}$$

For $q \ll 1$, we observe $S(\boldsymbol{q}) \sim q^2$: the large-scale fluctuations are highly suppressed in the limit $T \to 0$, see Fig. 4. This anomalous suppression of the fluctuations is referred to as hyperuniformity [47]. Hyperuniformity was also reported in other periodically driven systems, such as chiral active matter [38,58] and pulsating epithelial tissues [42]. In previous theoretical works, the authors of Refs. [59,60] discussed that hyperuniformity of the chiral active matter is a consequence of the conservation of the center of mass [61]. Our model instead asserts that this phenomenon is induced by the periodic nature of the driving force. A recent theoretical calculation by the fluctuating hydrodynamics also supports this conclusion, see Ref. [62]. However, it is not necessary that all instances of hyperuniformity come from a single underlying cause. For instance, the long-range hydrodynamic interaction is another
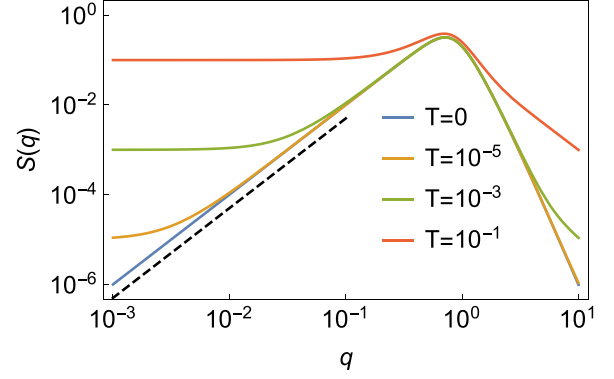

FIG. 4. $S(q)$ for model-B. The solid lines denote $S(q)$ for $T = 0, 10^{-5}, 10^{-3}, 10^{-1}$ from bottom to top. The black dashed line denotes $S(q) \propto q^2$. When $T = 0$, the model exhibits hyperuniformity $S(q) \propto q^2$ for $q \ll 1$. For simplicity, here we set $D = 1$, $\omega_0 = 1$, and $\mu = 1$.

source of hyperuniformity [38,63,64]. Further studies would be beneficial to elucidate this point.

When $\omega_0 = 0$, $S(\boldsymbol{q})$ shows the power-low divergence $S(q) \sim q^{-2}$ for $q \ll 1$, meaning that the large-scale fluctuations are significantly enhanced even in the disordered phase. The same power-low behavior was previously reported for the scalar active matter in quenched random potentials [65].

The Lagrange multiplier μ is to be determined by

$$1 = \frac{m^2}{\rho} + T F_B(\mu) + D G_B(\mu), \tag{37}$$

where $\rho = N/V$ and

$$F_B(\mu) = \frac{\Omega_d}{(2\pi)^d \rho} \int_0^{q_D} \frac{dq q^{d-1}}{q^2 + \mu},$$

$$G_B(\mu) = \frac{\Omega_d}{(2\pi)^d \rho} \int_0^{q_D} \frac{dq q^{d-1} q^2}{\omega_0^2 + q^4(q^2 + \mu)^2}. \tag{38}$$

Then, one can draw the critical line by $1 = m^2/\rho + T F_B(0) + D G_B(0)$ as in the case of the model-A. Note that m should be considered as the control parameter since the model-B dynamics conserves m. We here only discuss the behavior for $m = 0$. We show the phase diagrams in Figs. 1 to 3(b), and the lower critical dimension is

$$d_l = \begin{cases} 2 & T > 0, \quad \omega_0 \neq 0, \\ 0 & T = 0, \quad \omega_0 \neq 0, \\ 6 & \omega_0 = 0. \end{cases} \tag{39}$$

For $\omega_0 \neq 0$, the qualitative phase behaviors agree with that of the model-A. However, for $\omega_0 = 0$, $G_B(0)$ diverges for $d \leqslant 6$, leading to $d_l = 6$. Therefore, the ordered phase does not appear for $d \leqslant 6$, see Fig. 3(b). This result also consistent with the Imry-Ma argument for the continuous symmetry breaking of the active matter in quenched random fields [65].

V. SUMMARY AND DISCUSSIONS

In summary, we introduced and investigated the linear and spherical model driven by the temporally periodic but spatially inhomogeneous driving forces. We found that in the absence of the thermal noise, the lower critical dimension was $d_l = 0$, meaning that the models showed the continuous

symmetry breaking even in $d = 1$ and 2. Furthermore, the model for the conserved order parameter (model-B) showed hyperuniformity.

It is well known from the Imry-Ma argument that time-independent inhomogeneous external fields prohibit the continuous symmetry breaking for $d \leqslant 4$ [53]. One may expect that the time dependence of the external field introduced extra complexity, which made the system more disordered. However, our result demonstrated that the inhomogeneous oscillatory external field allowed the continuous symmetry breaking for $d \leqslant 4$.

It is also surprising that our model underwent continuous symmetry breaking even in $d = 1$. Although there were several known examples of nonequilibrium phase transitions in one dimension [46,61,66–69], the continuous symmetry breaking was hardly observed in $d = 1$, though our recent studies reported several other promising candidates [17,70].

To derive the lower critical dimension, Eq. (16), we only assumed the existence of the NG modes. Therefore, the result $d_l = 0$ should be generally applied for continuous symmetry breaking of periodically driven systems. For instance, our theory can be tested in crystal phases of chiral active particles [35,36] and actively deforming particles [32,71] by observing the translational order parameters. We hope our results will be verified in numerical simulations and experiments of those systems.

Note added. After the previous version was submitted, one of the authors confirmed that chiral active particles can indeed exhibit long-range crystalline order even in two dimensions [72].

[1] H. Nishimori and G. Ortiz, *Elements of Phase Transitions and Critical Phenomena* (Oxford University Press, Oxford, 2010).

[2] K. G. Wilson, Renormalization group and critical phenomena. I. Renormalization group and the Kadanoff scaling picture, Phys. Rev. B **4**, 3174 (1971).

[3] L. P. Kadanoff, Scaling laws for Ising models near T_c, Phys. Phys. Fiz. **2**, 263 (1966).

[4] L. Onsager, Crystal statistics. I. A two-dimensional model with an order-disorder transition, Phys. Rev. **65**, 117 (1944).

[5] S. G. Brush, History of the Lenz-Ising model, Rev. Mod. Phys. **39**, 883 (1967).

[6] B. J. Alder and T. E. Wainwright, Phase transition for a hard sphere system, J. Chem. Phys. **27**, 1208 (1957).

[7] K. Hukushima and K. Nemoto, Exchange Monte Carlo method and application to spin glass simulations, J. Phys. Soc. Jpn. **65**, 1604 (1996).

[8] D. Frenkel and B. Smit, *Understanding Molecular Simulation: From Algorithms to Applications* (Elsevier, Amsterdam, 2001), Vol. 1.

[9] N. D. Mermin and H. Wagner, Absence of ferromagnetism or antiferromagnetism in one- or two-dimensional isotropic Heisenberg models, Phys. Rev. Lett. **17**, 1133 (1966).

[10] P. C. Hohenberg, Existence of long-range order in one and two dimensions, Phys. Rev. **158**, 383 (1967).

[11] K. E. Bassler and Z. Rácz, Existence of long-range order in the steady state of a two-dimensional, two-temperature XY model, Phys. Rev. E **52**, R9 (1995).

[12] M. D. Reichl, C. I. Del Genio, and K. E. Bassler, Phase diagram for a two-dimensional, two-temperature, diffusive XY model, Phys. Rev. E **82**, 040102(R) (2010).

[13] F. Corberi, E. Lippiello, and M. Zannetti, Slow relaxation in the large-n model for phase ordering, Phys. Rev. E **65**, 046136 (2002).

[14] H. Nakano, Y. Minami, and S. Sasa, Long-range phase order in two dimensions under shear flow, Phys. Rev. Lett. **126**, 160604 (2021).

[15] H. Ikeda, Scaling theory of continuous symmetry breaking under advection, arXiv:2401.01603.

[16] L. Galliano, M. E. Cates, and L. Berthier, Two-dimensional crystals far from equilibrium, Phys. Rev. Lett. **131**, 047101 (2023).

[17] H. Ikeda, Correlated noise and critical dimensions, Phys. Rev. E **108**, 064119 (2023).

[18] T. Vicsek, A. Czirók, E. Ben-Jacob, I. Cohen, and O. Shochet, Novel type of phase transition in a system of self-driven particles, Phys. Rev. Lett. **75**, 1226 (1995).

[19] J. Toner and Y. Tu, Long-range order in a two-dimensional dynamical XY model: How birds fly together, Phys. Rev. Lett. **75**, 4326 (1995).

[20] H. Ikeda, Minimum scaling model and exact exponents for the Nambu-Goldstone modes in the vicsek model, arXiv:2403.02086.

[21] S. A. M. Loos, S. H. L. Klapp, and T. Martynec, Long-range order and directional defect propagation in the nonreciprocal *XY* model with vision cone interactions, Phys. Rev. Lett. **130**, 198301 (2023).

[22] L. P. Dadhichi, J. Kethapelli, R. Chajwa, S. Ramaswamy, and A. Maitra, Nonmutual torques and the unimportance of motility for long-range order in two-dimensional flocks, Phys. Rev. E **101**, 052601 (2020).

[23] M. Rao, H. R. Krishnamurthy, and R. Pandit, Hysteresis in model spin systems, J. Phys.: Condens. Matter **1**, 9061 (1989).

[24] M. Rao, H. R. Krishnamurthy, and R. Pandit, Magnetic hysteresis in two model spin systems, Phys. Rev. B **42**, 856 (1990).

[25] D. Dhar and P. B. Thomas, Hysteresis and self-organized criticality in the O(N) model in the limit N to infinity, J. Phys. A: Math. Gen. **25**, 4967 (1992).

[26] P. B. Thomas and D. Dhar, Hysteresis in isotropic spin systems, J. Phys. A: Math. Gen. **26**, 3973 (1993).

[27] J. B. Knight, C. G. Fandrich, C. N. Lau, H. M. Jaeger, and S. R. Nagel, Density relaxation in a vibrated granular material, Phys. Rev. E **51**, 3957 (1995).

[28] P. Hébraud, F. Lequeux, J. P. Munch, and D. J. Pine, Yielding and rearrangements in disordered emulsions, Phys. Rev. Lett. **78**, 4657 (1997).

[29] L. Berthier, L. F. Cugliandolo, and J. L. Iguain, Glassy systems under time-dependent driving forces: Application to slow granular rheology, Phys. Rev. E **63**, 051302 (2001).

[30] L. Berthier and J. Kurchan, Lectures on non-equilibrium active systems, arXiv:1906.04039.

[31] S. M. Zehnder, M. Suaris, M. M. Bellaire, and T. E. Angelini, Cell volume fluctuations in MDCK monolayers, Biophys. J. **108**, 247 (2015).

[32] E. Tjhung and L. Berthier, Discontinuous fluidization transition in time-correlated assemblies of actively deforming particles, Phys. Rev. E **96**, 050601(R) (2017).

[33] S. van Teeffelen and H. Löwen, Dynamics of a Brownian circle swimmer, Phys. Rev. E **78**, 020101(R) (2008).

[34] V. E. Debets, H. Löwen, and L. M. C. Janssen, Glassy dynamics in chiral fluids, Phys. Rev. Lett. **130**, 058201 (2023).

[35] A. Callegari and G. Volpe, Numerical simulations of active brownian particles, in *Flowing Matter*, edited by F. Toschi and M. Sega (Springer, Cham, Germany, 2019), pp. 211–238.

[36] B. Liebchen and D. Levis, Chiral active matter, Europhys. Lett. **139**, 67001 (2022).

[37] Z.-F. Huang, A. M. Menzel, and H. Löwen, Dynamical crystallites of active chiral particles, Phys. Rev. Lett. **125**, 218002 (2020).

[38] M. Huang, W. Hu, S. Yang, Q.-X. Liu, and H. P. Zhang, Circular swimming motility and disordered hyperuniform state in an algae system, Proc. Natl. Acad. Sci. USA **118**, e2100493118 (2021).

[39] F.-J. Lin, J.-J. Liao, and B.-Q. Ai, Spontaneous crystallization of chiral active colloidal particles, Physica A **608**, 128312 (2022).

[40] V. Semwal, J. Joshi, and S. Mishra, Macro to micro phase separation in a collection of chiral active swimmers, arXiv:2208.09448.

[41] Y. Zhang and É. Fodor, Pulsating active matter, Phys. Rev. Lett. **131**, 238302 (2023).

[42] Z.-Q. Li, Q.-L. Lei, and Y. qiang Ma, Fluidization and anomalous density fluctuations in epithelial tissues with pulsating activity, arXiv:2402.02981.

[43] G. S. Joyce, Spherical model with long-range ferromagnetic interactions, Phys. Rev. **146**, 349 (1966).

[44] T. H. Berlin and M. Kac, The spherical model of a ferromagnet, Phys. Rev. **86**, 821 (1952).

[45] H. E. Stanley, Spherical model as the limit of infinite spin dimensionality, Phys. Rev. **176**, 718 (1968).

[46] M. Henkel, H. Hinrichsen, S. Lübeck, and M. Pleimling, *Non-Equilibrium Phase Transitions* (Springer, New York, 2008), Vol. 1.

[47] S. Torquato, Hyperuniform states of matter, Phys. Rep. **745**, 1 (2018).

[48] Y. Nambu, Quasi-particles and gauge invariance in the theory of superconductivity, Phys. Rev. **117**, 648 (1960).

[49] J. Goldstone, A. Salam, and S. Weinberg, Broken symmetries, Phys. Rev. **127**, 965 (1962).

[50] R. Zwanzig, *Nonequilibrium Statistical Mechanics* (Oxford University Press, Oxford, 2001).

[51] E. Medina, T. Hwa, M. Kardar, and Y.-C. Zhang, Burgers equation with correlated noise: Renormalization-group analysis and applications to directed polymers and interface growth, Phys. Rev. A **39**, 3053 (1989).

[52] C. Maggi, N. Gnan, M. Paoluzzi, E. Zaccarelli, and A. Crisanti, Critical active dynamics is captured by a colored-noise driven field theory, Commun. Phys. **5**, 55 (2022).

[53] Y. Imry and S. Ma, Random-field instability of the ordered state of continuous symmetry, Phys. Rev. Lett. **35**, 1399 (1975).

[54] P. C. Hohenberg and B. I. Halperin, Theory of dynamic critical phenomena, Rev. Mod. Phys. **49**, 435 (1977).

[55] A. Crisanti, A. Sarracino, and M. Zannetti, Condensation versus ordering: From the spherical models to Bose-Einstein condensation in the canonical and grand canonical ensemble, Phys. Rev. Res. **1**, 023022 (2019).

[56] A. Onuki, *Phase Transition Dynamics* (Cambridge University Press, Cambridge, England, 2002).

[57] M. E. Cates, Active field theories, arXiv:1904.01330.

[58] B. Zhang and A. Snezhko, Hyperuniform active chiral fluids with tunable internal structure, Phys. Rev. Lett. **128**, 218002 (2022).

[59] Q.-L. Lei and R. Ni, Hydrodynamics of random-organizing hyperuniform fluids, Proc. Natl. Acad. Sci. USA **116**, 22983 (2019).

[60] Q.-L. Lei, M. P. Ciamarra, and R. Ni, Nonequilibrium strongly hyperuniform fluids of circle active particles with large local density fluctuations, Sci. Adv. **5**, eaau7423 (2019).

[61] D. Hexner and D. Levine, Noise, diffusion, and hyperuniformity, Phys. Rev. Lett. **118**, 020601 (2017).

[62] Y. Kuroda and K. Miyazaki, Microscopic theory for hyperuniformity in two-dimensional chiral active fluid, J. Stat. Mech.: Theory Exp. (2023) 103203.

[63] S. Torquato, Swimming in circles can lead to exotic hyperuniform states of active living matter, Proc. Natl. Acad. Sci. USA **118**, e2107276118 (2021).

[64] N. Oppenheimer, D. B Stein, M. Y. B. Zion, and M. J. Shelley, Hyperuniformity and phase enrichment in vortex and rotor assemblies, Nat. Commun. **13**, 804 (2022).

[65] S. Ro, Y. Kafri, M. Kardar, and J. Tailleur, Disorder-induced long-ranged correlations in scalar active matter, Phys. Rev. Lett. **126**, 048003 (2021).

[66] A. Czirók, A.-L. Barabási, and T. Vicsek, Collective motion of self-propelled particles: Kinetic phase transition in one dimension, Phys. Rev. Lett. **82**, 209 (1999).

[67] O. J. OLoan and M. R. Evans, Alternating steady state in one-dimensional flocking, J. Phys. A: Math. Gen. **32**, L99 (1999).

[68] A. P. Solon and J. Tailleur, Revisiting the flocking transition using active spins, Phys. Rev. Lett. **111**, 078101 (2013).

[69] M. R. Evans and T. Hanney, Nonequilibrium statistical mechanics of the zero-range process and related models, J. Phys. A: Math. Gen. **38**, R195 (2005).

[70] H. Ikeda, Harmonic chain far from equilibrium: single-file diffusion, long-range order, and hyperuniformity, arXiv:2309.03155.

[71] D. R. Parisi, L. E. Wiebke, J. N. Mandl, and J. Textor, Flow rate resonance of actively deforming particles, Sci. Rep. **13**, 9455 (2023).

[72] Y. Kuroda, T. Kawasaki, and K. Miyazaki, Long-range translational order and hyperuniformity in two-dimensional chiral active crystal, arXiv:2402.19192.